1566 *Inorg. Chem.* **1992**, *31*, 1566–1574

Contribution from the Department of Chemistry and Biochemistry, University of Notre Dame, Notre Dame, Indiana 46556, and Department of Chemistry, Faculty of Science, Shizuoka University, Ohya, Shizuoka 422, Japan

Transient Chiral Induction in the Reactions of Optically Active $[Co(ox)_3]^{3-}$ with $[Co(phen)_3]^{2+}$ and Derivatives

Robert M. L. Warren,[1] A. Graham Lappin,*[,1] and Akira Tatehata*[,2]

Received September 12, 1991

The kinetics of reduction of $[Co(ox)_3]^{3-}$ by $[Co(phen)_3]^{2+}$ (ox^{2-} = oxalate(2−), phen = 1,10-phenanthroline) were investigated under pseudo-first-order conditions with an excess of reductant at 25.0 °C and 0.017 M ionic strength. At low $[[Co(phen)_3]^{2+}]$ the reaction is first order in both reactants, with a second-order rate constant, $k_{os} = 15.8\ M^{-1}\ s^{-1}$ ($\Delta H^* = 12.1$ kJ mol^{-1}, $\Delta S^* = -181$ J K^{-1} mol^{-1}). The rate shows limiting first-order behavior at higher $[[Co(phen)_3]^{2+}]$, consistent with an outer-sphere mechanism involving a kinetically significant ion pair. The ion-association constant for formation of this ion pair is calculated to be 65 M^{-1} ($\Delta H^\circ = -20$ kJ mol^{-1}, $\Delta S^\circ = -33$ J K^{-1} mol^{-1}), and the limiting first-order electron-transfer rate is 0.24 s^{-1} ($\Delta H_{et}^* = 32$ kJ mol^{-1}, $\Delta S_{et}^* = -148$ J K^{-1} mol^{-1}). As [phen] is reduced so that $[Co(phen)_2]^{2+}$ predominates, a second, inner-sphere pathway is revealed. In this pathway, a doubly bridged oxalate group is transferred from $[Co(ox)_3]^{3-}$ to $[Co(phen)_2]^{2+}$ with $k_{is} = 94\ M^{-1}\ s^{-1}$ to give $[Co(phen)_2(ox)]^+$ as the initial product. Both outer-sphere and inner-sphere processes show significant overall stereoselectivities with $k_{os}(\Delta\Delta)/k_{os}(\Delta\Lambda) = 1.63$ and $k_{is}(\Delta\Delta)/k_{is}(\Delta\Lambda) = 4.4$, respectively. Less extensive studies have also been carried out on the reduction of $[Co(ox)_3]^{3-}$ by $[Co(bpy)_3]^{2+}$, $[Co(4,7\text{-}Me_2phen)_3]^{2+}$, and $[Co(5,6\text{-}Me_2phen)_3]^{2+}$ (bpy = 2,2′-bipyridyl). Information on stereoselectivity in the ion pair formed between $[Co(ox)_3]^{3-}$ and $[Co(phen)_3]^{2+}$ was investigated with conductivity studies on the analogues $[Rh(ox)_3]^{3-}$ and $[Ru(phen)_3]^{2+}$. At 0.010 M ionic strength and 25.0 °C, there is little difference in ion-association constants for the diastereomeric ion pairs with $K_0(\Delta\Delta)/K_0(\Delta\Lambda) = 1.05$. Consequently, it is argued that most of the chiral discrimination in the outer-sphere electron-transfer pathway occurs in the intramolecular electron-transfer step within the ion pair. NMR studies and crystallographic data from related systems suggest that despite the small diastereomeric discrimination, the ion pair shows a significant degree of structure, with metal centers ≈6 Å apart and with a predominant C_3–C_3 interaction. The dependence of stereoselectivity on reductant structure is consistent with this model. The self-exchange rate for $[Co(bpy)_3]^{3+/2+}$ was also determined to be 5.7 M^{-1} s^{-1} ($\Delta H^* = 31.1$ kJ mol^{-1}, $\Delta S^* = -127$ J K^{-1} mol^{-1}) at 25.0 °C and 0.10 M ionic strength.

Introduction

Stereoselectivity in outer-sphere electron-transfer reactions between transition metal ion complexes has been the subject of a number of investigations over the past decade.[3-8] The phenomenon appears to be quite general[9] although technical difficulties associated with measuring small rate differences or the characterization of kinetic products may prevent detection. In most instances, stereoselectivities are not large but they do show a marked variation with the structures and charges of the reactants and the reaction medium, features which recommend stereoselectivity as an important probe of mechanism. However, interpretation of the data is often difficult.

It has been convenient to focus discussion of the stereoselectivity on the structures of intermediates in the electron-transfer process and particularly on structures of precursor complexes. Steric and directional binding forces such as hydrogen bonding play an important role in chiral recognition in ion association,[10-12] and this is reflected in the chiral induction in electron-transfer reactions.[5-8] Indeed, in outer-sphere processes where these features are dominant, there are strong correlations between chiral induction in the electron transfer and chiral recognition in ion association between nonredox-active analogues.[5,9] In these instances, it can be concluded that the ion-pairing interactions model those of the electron-transfer precursor. It is much more difficult to investigate factors which influence stereoselectivity in the nuclear reorganization associated with the electron-transfer step itself, despite a number of arguments which suggest that such factors can be very important.[5,13]

Direct experimental evidence for an important role for these factors has been obtained by Saito and co-workers[4] in a reaction where the ion-pair formation and electron-transfer steps are kinetically distinct. The extent of the stereoselectivity is very small, but chiral recognition in the ion pair is in the opposite sense to that in the electron transfer. Bernauer and co-workers[14] have suggested, on the basis of an analysis of activation parameters, that strong chiral recognition may result in slower electron transfer. In order to examine this problem further, a detailed study of the oxidation of $[Co(phen)_3]^{2+}$ by $[Co(ox)_3]^{3-}$ has been undertaken. Ion-pair formation is expected to be significant, but strongly directional hydrogen-bonding forces are absent, and the high symmetry of the reacting species should simplify interpretation of the data. Stereoselectivity studies are complicated because the reaction product, $[Co(phen)_3]^{3+}$, undergoes self-exchange catalyzed racemization in the presence of $[Co(phen)_3]^{2+}$, and consequently any chiral induction is transitory. Details of the electron-transfer-catalyzed racemization of $[Co(phen)_3]^{3+}$ and of a number of structural variants have been published previously and are well understood.[15] The oxidation of $[Co(bpy)_3]^{2+}$ by $[Co(ox)_3]^{3-}$ and electron-transfer-catalyzed racemization of $[Co(bpy)_3]^{3+}$ by $[Co(bpy)_3]^{2+}$ are also included in the present study.

Experimental Section

(a) Materials. $K_3[Rh(ox)_3]\cdot 4.5H_2O$ was prepared[16] from freshly precipitated rhodium hydroxide and potassium hydrogen oxalate, purified by the method of Barton and Harris[17] and resolved[18] with use of Λ-$(+)_{589}$-$[Ni(phen)_3](ClO_4)_2\cdot 3H_2O$ or chiral $[Ni(phen)_3]I_2$. The absolute configuration is $K_3\Lambda$-$(+)_{546}$-$[Rh(ox)_3]\cdot 2H_2O$ ($\epsilon_{402} = 330\ M^{-1}\ cm^{-1}$, $\Delta\epsilon_{400} = +2.85\ M^{-1}\ cm^{-1}$).[19] The $\Delta\epsilon$ values at 398 nm for the $(+)_{546}$ and $(-)_{546}$ isomers were +2.85 and −2.88 M^{-1} cm^{-1}, respectively. $[Ru(phen)_3]Cl_2\cdot 6H_2O$ was purchased from Alfa or Aldrich and recrystallized (typically ×3).[20] It was resolved by the method of Dwyer and Gyarfas,[21]

---

(1) University of Notre Dame.

(2) Shizuoka University.

(3) Geselowitz, D. A.; Taube, H. *J. Am. Chem. Soc.* **1980**, *102*, 4525–4526.

(4) Kondo, S.; Sasaki, Y.; Saito, K. *Inorg. Chem.* **1981**, *20*, 429–433.

(5) Osvath, P.; Lappin, A. G. *Inorg. Chem.* **1987**, *26*, 195–202.

(6) Geselowitz, D. A.; Hammershøi, A.; Taube, H. *Inorg. Chem.* **1987**, *26*, 1842–1845.

(7) Marusak, R. A.; Osvath, P.; Kemper, M.; Lappin, A. G. *Inorg. Chem.* **1989**, *28*, 1542–1548.

(8) Tatehata, A.; Mitani, T. *Chem. Lett.* **1989**, 1167–1170.

(9) Lappin, A. G.; Marusak, R. A. *Coord. Chem. Rev.* **1991**, *109*, 125–180.

(10) Tatehata, A.; Fujita, M.; Ando, K.; Asaba, Y. *J. Chem. Soc., Dalton Trans.* **1987**, 1977–1982.

(11) Tatehata, A.; Asaba, Y. *Bull. Chem. Soc. Jpn.* **1988**, *61*, 3145–3151.

(12) Miyoshi, K.; Sakamoto, Y.; Ohguni, A.; Yoneda, H. *Bull. Chem. Soc. Jpn.* **1985**, *58*, 2239–2246.

(13) Pispisa, B.; Palleschi, A.; Paradossi, G. *J. Phys. Chem.* **1987**, *91*, 1546–1553.

(14) Bernauer, K.; Monzione, M.; Schürmann, P.; Viette, V. *Helv. Chim. Acta* **1990**, *73*, 346–352.

(15) Warren, R. M. L.; Lappin, A. G.; Mehta, B. D.; Neumann, H. M. *Inorg. Chem.* **1990**, *29*, 4185–4189.

(16) Werner, A.; Poupardin, J. *Berichte* **1914**, *47*, 1954–1960.

(17) Barton, D.; Harris, G. M. *Inorg. Chem.* **1962**, *1*, 251–255.

(18) Dwyer, F. P.; Sargeson, A. M. *J. Phys. Chem.* **1956**, *60*, 1331–1332.

(19) McCaffery, A. J.; Mason, S. F.; Ballard, R. E. *J. Chem. Soc.* **1965**, 2883–2892.

(20) Broomhead, J. A.; Young, C. G. *Inorg. Synth.* **1982**, *21*, 127–128.

0020-1669/92/1331-1566\$03.00/0

Table I. Stepwise Stability and Acidity Constants for Cobalt(II) Complexes with 2,2′-Bipyridine, 1,10-Phenanthroline, and Its Substituted Derivatives and Reduction Potential Data for the Tris-Cobalt(III) Complexes, at 25.0 °C and 0.10 M Ionic Strength[33]

ligand	log K_1	log K_2	log K_3	pK_{a1}	$E°$, mV
phen	6.96	6.73	6.08	4.98	355
bpy	5.65	5.60	4.80	4.47	310
4,7-Me$_2$phen	8.08	8.00	8.43	5.95	160
5,6-Me$_2$phen	7.47	8.00	8.14	5.60	230

to produce the perchlorate salt. The absolute configuration is Λ-$(+)_{589}$-$[Ru(phen)_3](ClO_4)_2\cdot H_2O$ (ϵ_{262} = 89 000 M^{-1} cm^{-1}, $\Delta\epsilon_{267}$ = +540 M^{-1} cm^{-1}, $\Delta\epsilon_{257}$ = −410 M^{-1} cm^{-1}).[22] The chloride salt was obtained by elution on a Dowex 1X8-100 anion-exchange resin in the chloride form, and the bromide salt, with use of a column of DEAE-Sephadex A-25 resin in the bromide form. Solutions eluted from the column were concentrated almost to dryness and dissolved in ethanol, and the products were isolated by adding ethyl ether. The $[\alpha]_{589}$ values obtained for the $(+)_{589}$ and $(-)_{589}$ isomers in the present study were +1360 and −1350°, respectively. The syntheses of $[Co(phen)_3]Cl_3\cdot 7H_2O$,[15] Δ-$(-)_{589}$-$[Co(bpy)_3](ClO_4)_3\cdot 2H_2O$ (ϵ_{450} = 71.5 M^{-1} cm^{-1}, $\Delta\epsilon_{449}$ = +3.05 M^{-1} cm^{-1}),[23] $[Co(phen)_2(ox)]Cl\cdot 4H_2O$ (ϵ_{508} = 77.3 M^{-1} cm^{-1}),[24] and $[Co(bpy)_2(ox)]Cl\cdot 4H_2O$ (ϵ_{499} = 81.3 M^{-1} cm^{-1})[24] were carried out as described in the literature. The absolute configurations of the latter two complexes are Δ-(−)-$[Co(phen)_2(ox)]ClO_4\cdot H_2O$ ($\Delta\epsilon_{520}$ = −0.99 M^{-1} cm^{-1}) and Δ-(−)-$[Co(bpy)_2(ox)]ClO_4\cdot H_2O$ ($\Delta\epsilon_{525}$ = −2.15 M^{-1} cm^{-1}).[24,25] $K_3[Co(ox)_3]\cdot 3.5H_2O$[26] was used to prepare $K_3\Delta$-$(+)_{589}$-$[Co(ox)_3]\cdot 3.5H_2O$ (ϵ_{605} = 165 M^{-1} cm^{-1}, $\Delta\epsilon_{622}$ = −3.80 M^{-1} cm^{-1})[27–29] by the method of Kaufman and co-workers.[30] Both racemic and optically active salts were purified by reprecipitation from alcohol, and purities were checked spectrophotometrically before each experiment. All manipulations involving this complex were carried out in subdued light, and all results were corrected for racemization by determining the optical purity of solutions before and after use. $K_3[Cr(ox)_3]\cdot 3H_2O$ (ϵ_{571} = 74 M^{-1} cm^{-1})[19] was prepared by the method of Bailar and Jones.[26]

The macrocycles 1,4,7,10,13,16-hexaoxacyclooctadecane (18-crown-6, Aldrich, $K_{K^+} = 10^{2.03}$)[31] and 4,7,13,16,21,24-hexaoxa-1,10-diazabicyclo[8.8.8]hexacosane ([2.2.2] cryptand, Fluka, $K_{K^+} = 10^{5.4}$, pK_{a1} = 9.60, pK_{a2} = 7.28)[32] were used as received. The ligands 1,10-phenanthroline monohydrate (phen, Fluka) and 2,2′-bipyridine (bpy, Strem or Aldrich) were used as received. 4,7-Dimethyl-1,10-phenanthroline (4,7-Me$_2$phen, G. F. Smith) and 5,6-dimethyl-1,10-phenanthroline (5,6-Me$_2$phen, G. F. Smith) were purified as described previously.[15] Stability and acidity constants for these ligands and reduction potentials for the complexes are given in Table I.[33] Solutions of $[Co(phen)_3]^{2+}$ and the other labile tris-ligand cobalt(II) complexes were prepared from $Co(NO_3)_2\cdot 6H_2O$ (Baker Analyzed) with a concentration of ligand in sufficient excess to form ≥99% of the tris species. The magnitudes of the stability constants for the ligands do not allow quantitative formation of the bis complexes such as $[Co(phen)_2]^{2+}$. However, with [Co(II)]:[phen] = 1:2 and cobalt(II) concentrations of 1 × 10^{-3} M, approximately 49% of the species exists as $[Co(phen)_2]^{2+}$, while 28% exists as $[Co(phen)_3]^{2+}$. For the complexes of bpy, the corresponding percentages are 53% as $[Co(bpy)_2]^{2+}$ and 26% as $[Co(bpy)_3]^{2+}$. Cobalt(II) ion concentrations were determined spectrophotometrically before the addition of the free ligand ($[Co(H_2O)_6]^{2+}$, ϵ_{509} = 4.84 M^{-1} cm^{-1}).[34] All solutions were prepared and used under an atmosphere of argon gas. In particular, solutions of $[Co(5,6\text{-}Me_2phen)_3]^{2+}$, $[Co(4,7\text{-}Me_2phen)_3]^{2+}$, and to a lesser extent $[Co(bpy)_3]^{2+}$ are susceptible to autoxidation.[35] Nitrate salts of lithium, sodium, and potassium (Baker Analyzed) were added to solutions to adjust the ionic strength as necessary. The buffers *N*-morpholineethanesulfonic acid (MES), tris(hydroxymethyl)aminomethane (TRIS), 3-(cyclohexylamino)-1-propanesulfonic acid (CAPS), and 3-(cyclohexylamino)-2-hydroxy-1-propanesulfonic acid (CAPSO) were purchased from Sigma. All solutions were prepared immediately before use.

Table II. Limiting Equivalent Conductivities (S cm^2 equiv^{-1})

complex salt	Λ_0	λ_{0^+}	λ_{0^-}
Λ-$(+)_{589}$-$[Ru(phen)_3]Br_2$	113.03	34.89	78.14[a]
Δ-$(-)_{589}$-$[Ru(phen)_3]Br_2$	113.22	35.08	78.14[a]
Λ-$(+)_{546}$-$K_3[Rh(ox)_3]$	156.80	73.50[a]	83.30
Δ-$(-)_{546}$-$K_3[Rh(ox)_3]$	156.86	73.50[a]	83.36

[a] Reference 38.

(b) Methods. The kinetics of reduction of $[Co(ox)_3]^{3-}$ by $[Co(phen)_3]^{2+}$ and its derivatives were investigated under pseudo-first-order conditions with a 10-fold or greater excess of reductant. For most studies the ionic strength was 0.017 M, with an oxidant concentration of 2 × 10^{-5} M and a reductant concentration of 2 × 10^{-4}–6 × 10^{-3} M. Buffer concentrations were 10^{-3}–10^{-2} M. Reactions of $[Co(ox)_3]^{3-}$ were monitored by observing the decrease in absorbance of the oxidant at 605 nm. The reduction of $[Co(phen)_2(ox)]^+$ by $[Co(phen)_3]^{2+}$ was monitored at 530 nm, and that of $[Co(bpy)_2(ox)]^+$ by $[Co(bpy)_3]^{2+}$ at 520 nm, again following the decrease in absorbance due to the oxidant. Plots of ln $(A - A_\infty)$ were generally linear for at least 3 half-lives, and pseudo-first-order rate constants, k_{obsd}, were calculated from the slopes by least-squares analysis. The pseudo-first-order rate constants are collected in Table SI, available as supplementary material. Conventional kinetics were monitored on a Varian DMS-100 UV–visible spectrophotometer equipped with a water-jacketed cell holder, giving temperature control to better than ±0.2 °C. Stopped-flow kinetics were run on a Durrum D-110 stopped-flow spectrophotometer, modified to enable solutions to be handled under an atmosphere of argon and thermostated at 25.0 ± 0.1 °C. The pH was measured immediately after each reaction with a Beckman SelectIon 2000 meter equipped with a Corning combination glass electrode with a saturated calomel (NaCl) reference.

The rate of racemization of Δ-$(-)_{589}$-$[Co(bpy)_3]^{3+}$, catalyzed by $[Co(bpy)_3]^{2+}$, was measured by observing the decay of the circular dichroism signal, ϕ, at 449 nm. The cobalt(III) concentration was maintained at 7.5 × 10^{-5} M, and the cobalt(II) concentrations were varied in the range (2–10) × 10^{-4} M. The reaction is first-order in both cobalt(III) and cobalt(II) concentration over this range of conditions. Plots of ln $(\phi - \phi_\infty)$ were generally linear for at least 3 half-lives, and first-order rate constants, k_{obsd}, were calculated from the slopes by least-squares analysis. The first-order rate constants are collected in Table SII, available as supplementary material. All circular dichroism measurements were made on an Aviv Model 60DS circular dichroism spectropolarimeter calibrated against an aqueous solution of Λ-$(+)_{589}$-$[Co(en)_3]Cl_3$ ($\Delta\epsilon_{493}$ = 1.90 M^{-1} cm^{-1}).[36] The instrument was equipped with a water-jacketed cell holder, giving temperature control to better than ±0.2 °C.

The stereoselectivity of the reduction of Δ-$(+)_{589}$-$[Co(ox)_3]^{3-}$ by each reductant was obtained by observing the circular dichroism response of the reaction at the following wavelengths: 487 and 435 nm for $[Co(phen)_3]^{2+}$, 449 nm for $[Co(bpy)_3]^{2+}$, 480 nm for $[Co(4,7\text{-}Me_2phen)_3]^{2+}$, 480 nm for $[Co(5,6\text{-}Me_2phen)_3]^{2+}$, 520 and 417 nm for $[Co(phen)_2]^{2+}$, and 525 and 487 nm for $[Co(bpy)_2]^{2+}$. Measurements were made using a 10-cm path length cell thermostated as described above. Typically, the concentration of the optically active oxidant was 1 × 10^{-4} M with the reductant in 10-fold excess. An excess is required since the rate of racemization of $[Co(phen)_3]^{2+}$ (6.9 s^{-1})[37] and presumably also of $[Co(bpy)_3]^{2+}$ is not sufficiently fast to allow continuous regeneration of the racemate in the faster reactions. Furthermore, isolation of optically active $[Co(phen)_3]^{3+}$ or $[Co(bpy)_3]^{3+}$ is not possible, since they are rapidly racemized[15] by the excess $[Co(phen)_3]^{2+}$ or $[Co(bpy)_3]^{2+}$, respectively. Optical activity from these species can however be detected as a transient, provided the redox process is significantly faster than the subsequent racemization. Such conditions are optimized by the low ionic strength used in this study.

NMR spectra were accumulated on a Nicolet NT-300 MHz instrument at 25.0 ± 0.5 °C. T_1 determinations were carried out using an inversion-recovery program. This employs the usual 180°–τ–90° pulse

---

(21) Dwyer, F. P.; Gyarfas, E. C. *J. Proc. R. Soc. New South Wales* **1949**, *83*, 170–173.
(22) Mason, S. F.; Peart, B. J. *J. Chem. Soc., Dalton Trans.* **1973**, 949–955.
(23) Ferguson, J.; Hawkins, C. J.; Kane-Maguire, N. A. P.; Lip, H. *Inorg. Chem.* **1969**, *8*, 771–779.
(24) Broomhead, J. A.; Dwyer, M.; Kane-Maguire, N. A. P. *Inorg. Chem.* **1968**, *7*, 1388–1393.
(25) Mason, S. F. *Inorg. Chim. Acta Rev.* **1968**, *2*, 89–109.
(26) Bailar, J. C.; Jones, E. M. *Inorg. Synth.* **1939**, *1*, 37.
(27) Sisley, M. J.; Segal, M. G.; Stanley, C. S.; Adzamli, I. K.; Sykes, A. G. *J. Am. Chem. Soc.* **1983**, *105*, 225–228.
(28) Okazaki, H.; Kushi, Y.; Yoneda, H. *J. Am. Chem. Soc.* **1985**, *107*, 4183–4189.
(29) Butler, K. R.; Snow, M. R. *J. Chem. Soc. A* **1971**, 565–569.
(30) Kaufman, G. B.; Takahashi, L. T.; Sugisaka, N. *Inorg. Synth.* **1966**, *8*, 208–209.
(31) Martell, A. E.; Smith, R. M. *Critical Stability Constants*; Plenum: New York, 1982; Vol. 5, p 369.
(32) Martell, A. E.; Smith, R. M. *Critical Stability Constants*; Plenum: New York, 1982; Vol. 5, p 191.
(33) McBryde, W. A. E. *IUPAC Chem. Data Ser.* **1978**, *17*, 18–36.
(34) Davies, G.; Watkins, K. O. *J. Phys. Chem.* **1970**, *74*, 3388–3392.
(35) Koval, C. A.; Pravata, R. L. A.; Reidsema, C. M. *Inorg. Chem.* **1984**, *23*, 545–553.
(36) McCaffery, A. J.; Mason, S. F.; Norman, B. J.; Sargeson, A. M. *J. Chem. Soc. A* **1968**, 1304–1310.
(37) Blinn, E. L.; Wilkins, R. G. *Inorg. Chem.* **1976**, *15*, 2952.

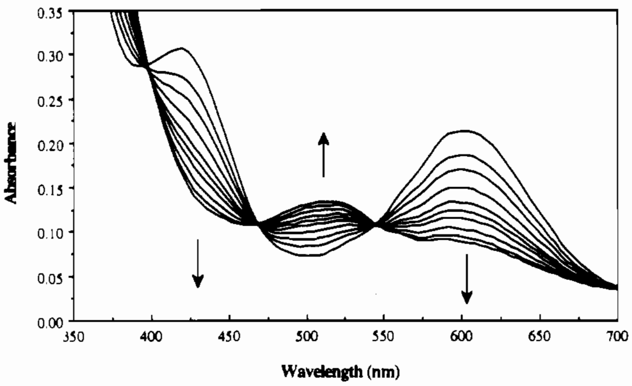

Figure 1. Absorbance changes during the reaction between 1.13 × 10^{-4} M $[Co(phen)_2]^{2+}$ and 1.08 × 10^{-4} M $[Co(ox)_3]^{3-}$ (pH 7.0 (TRIS buffer), 0.017 M ionic strength (KNO_3), 25.0 °C).

sequence, where τ is the delay time. At least 11 different delay times were used in each experiment. Spin–lattice relaxation rates were evaluated by plotting ln $(I_0 - I)$ versus τ and calculating the slopes $(-1/T_1)$ by least-squares analysis. All solutions for NMR studies were prepared with Cambridge Isotope Laboratories 99.9% D_2O under an atmosphere of argon gas to eliminate any effect of paramagnetic oxygen on the relaxation times.

Conductivity measurements were made at 25.00 ± 0.02 °C with use of a conductometer (Model MY-8 from Yanagimoto Mfg. Co. Ltd.) with a frequency of 800 Hz. To obtain the limiting equivalent conductivity, Λ_0, of the complex salts, plots of Λ against $(2[[Ru(phen)_3]^{2+}])^{1/2}$ were made for $(+)_{589}$- and $(-)_{589}$-$[Ru(phen)_3]Br_2$ and of Λ against $(3[[Rh(ox)_3]^{3-}])^{1/2}$ for $(+)_{546}$- and $(-)_{546}$-$K_3[Rh(ox)_3]$. From the Λ_0 values of the complex salts and Kohlrausch's law of the independent migration of ions, the limiting equivalent conductivities of the complex ions obtained, $\lambda_0([Ru(phen)_3]^{2+})$ and $\lambda_0([Rh(ox)_3]^{3-})$, are given in Table II. In the determination of ion-pairing constants, solutions with a stoichiometrically constant ionic strength were prepared by mixing solutions of chiral $[Ru(phen)_3]Br_2$ or $[Ru(phen)_3]Cl_2$ and chiral $K_3[Rh(ox)_3]$ both at the required ionic strength to give volume fractions χ and $1 - \chi$, respectively. For experiments at ionic strength 0.017 M and variable temperature, a Radiometer CDM80 conductivity meter operating at 3000 Hz and equipped with a CDC104 conductivity cell was used. The instrument was thermostated with a water-jacketed cell holder, giving temperature control to better than ±0.1 °C. Conductivity water (<0.7 μS cm^{-1}) was used for all measurements.

Results

(a) Stoichiometry of the Reaction between $[Co(ox)_3]^{3-}$ and $[Co(phen)_3]^{2+}$. In the reduction of $[Co(ox)_3]^{3-}$ by an excess of $[Co(phen)_3]^{2+}$, 0.95 ± 0.07 equiv of the sole isolable product, $[Co(phen)_3]^{3+}$, is produced for each 1 equiv of $[Co(ox)_3]^{3-}$ consumed (eq 1). When the reaction is carried out with solutions

$$[Co(phen)_3]^{2+} + [Co(ox)_3]^{3-} \rightarrow [Co(phen)_3]^{3+} + [Co(ox)_2]^{2-} + ox^{2-} \quad (1)$$

of lower [phen] concentrations where $[Co(phen)_2]^{2+}$ predominates, the behavior is more complex. The initial product formed has an absorption maximum around 510 nm (Figure 1), but under conditions of excess reductant, the final product is exclusively $[Co(phen)_3]^{3+}$, again with 1:1 stoichiometry. The intermediate is identified as $[Co(phen)_2(ox)]^+$, which has an absorption maximum at 508 nm. Small shifts in the isosbestic points during the course of the reaction are consistent with the direct formation of a small amount of $[Co(phen)_3]^{3+}$. The reaction with $[Co(bpy)_3]^{2+}$ shows similar behavior. $[Co(bpy)_3]^{3+}$ is the exclusive product where the reductant is $[Co(bpy)_3]^{2+}$, but at lower [bpy] concentrations, significant amounts of $[Co(bpy)_2(ox)]^+$ absorbing at 499 nm are formed initially.

(b) Kinetics of Reduction of $[Co(ox)_3]^{3-}$. At [phen] concentrations where ≥99% of the reductant is in the form $[Co(phen)_3]^{2+}$, plots of the pseudo-first-order rate constant for reduction of $[Co(ox)_3]^{3-}$, k_{obsd}, against $[[Co(phen)_3]^{2+}]$ are linear at low cobalt(II) concentrations but show limiting first-order behavior at higher cobalt(II) concentrations (Figure 2), as described by eq 2. This rate law is consistent with a mechanism[39] involving a

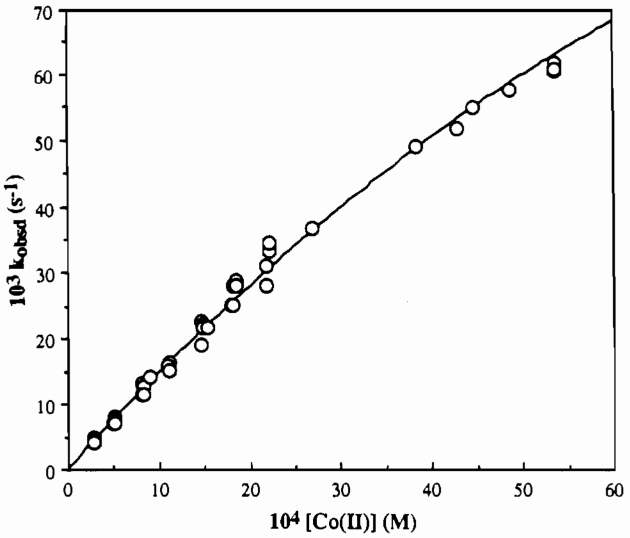

Figure 2. Plot of observed pseudo-first-order rate constant, k_{obsd}, against $[Co(phen)_3]^{2+}$ concentration for the reduction of $[Co(ox)_3]^{3-}$ by $[Co(phen)_3]^{2+}$ (0.017 M ionic strength (KNO_3), 25.0 °C).

$$k_{obsd} = \frac{k_{os}[[Co(phen)_3]^{2+}]}{1 + K_0[[Co(phen)_3]^{2+}]} \quad (2)$$

kinetically significant ion pair between the reactants (eqs 3 and 4), where the limiting first-order rate constant $k_{et} = k_{os}/K_0$. At

$$[Co(ox)_3]^{3-} + [Co(phen)_3]^{2+} \xrightleftharpoons{K_0} \{[Co(ox)_3]^{3-},[Co(phen)_3]^{2+}\} \quad (3)$$

$$\{[Co(ox)_3]^{3-},[Co(phen)_3]^{2+}\} \xrightarrow{k_{et}} \{[Co(ox)_3]^{4-},[Co(phen)_3]^{3+}\} \quad (4)$$

25.0 °C and 0.017 M ionic strength, the second-order rate constant k_{os} = 15.8 ± 0.3 M^{-1} s^{-1} and activation parameters determined over the temperature range 5–45 °C are $\Delta H^{\ddagger}$ = 12.1 ± 0.7 kJ mol^{-1} and $\Delta S^{\ddagger}$ = −181 ± 3 J K^{-1} mol^{-1}. The rate is independent of pH over the range 4–11, and there is no effect of changing buffer. The reaction was examined at 0.017 M ionic strength, pH 10.4, in $LiNO_3$, $NaNO_3$, KNO_3, and in KNO_3 with sufficient [2.2.2] cryptand added to complex out >99% of the K^+ cation. Second-order rate constants are 14.4 ± 1.2 M^{-1} s^{-1}, 16.6 ± 1.5 M^{-1} s^{-1}, 16.3 ± 1.6 M^{-1} s^{-1}, and 14.6 ± 1.8 M^{-1} s^{-1}, respectively, the same within experimental error. However, at higher concentrations of background electrolyte, a medium effect is observable[40] and the rate in $LiNO_3$ at 0.10 M ionic strength is 30% faster than in 0.10 M KNO_3. Analysis of the data in Figure 2 gives the ion association constant, K_0 = 65 ± 19 M^{-1} (ΔH° = −20 ± 2 kJ mol^{-1}, ΔS° = −33 ± 5 J K^{-1} mol^{-1}), and the limiting first-order electron-transfer rate constant, k_{et} = 0.24 ± 0.07 s^{-1} ($\Delta H_{et}^{\ddagger}$ = 32 ± 3 kJ mol^{-1}, $\Delta S_{et}^{\ddagger}$ = −148 ± 6 J K^{-1} mol^{-1}).

As [phen] is reduced so that $[Co(phen)_2]^{2+}$ predominates, the apparent second-order rate k_{so} increases (Table SI). The data as a function of added [phen] were fit to the expression (eq 5)

$$k_{so}[Co(II)]_T = k_{os}[[Co(phen)_3]^{2+}] + k_{is}[[Co(phen)_2]^{2+}] \quad (5)$$

by an iterative least-squares procedure, where k_{os} = 16 ± 2 M^{-1} s^{-1} is the second-order rate constant for reduction by $[Co(phen)_3]^{2+}$ and k_{is} = 94 ± 10 M^{-1} s^{-1} is the second-order rate constant for

---

(38) Robinson, R. A.; Stokes, R. H. *Electrolyte Solutions*, 2nd ed.; Butterworths: London, 1959; p 463.

(39) Deviations from second-order behavior may also be the result of medium effects, since at these low ionic strengths it is difficult to maintain a sensibly constant medium over the concentration range required for the kinetic investigations.

(40) Empirical fits to the data give $k_2 = 32.6/(1 + 68.5I)$ in KNO_3 media and $k_2 = (1 + 2.03I)/(0.031 + 2.03I)$ in $LiNO_3$ media, but the significance of these parameters is unclear.

Table III. Observed and Calculated Second-Order Rate Constants and Activation Parameters for the Reduction of $[Co(ox)_3]^{3-}$, $[Co(phen)_2(ox)]^+$, and $[Co(bpy)_2(ox)]^+$ with $[Co(phen)_3]^{2+}$ Derivatives at 25.0 °C and 0.017 M (KNO_3) Ionic Strength

reductant	oxidant	k_{so}, $M^{-1}\ s^{-1}$	k_{so}(calc),[a] $M^{-1}\ s^{-1}$	ΔH^*, kJ mol^{-1}	ΔS^*, J K^{-1} mol^{-1}
$[Co(phen)_3]^{2+}$	$[Co(ox)_3]^{3-}$	15.8 ± 0.3	15.8	12.1 ± 0.7	−181 ± 3
$[Co(phen)_2]^{2+}$	$[Co(ox)_3]^{3-}$	94 ± 10			
$[Co(bpy)_3]^{2+}$	$[Co(ox)_3]^{3-}$	50 ± 2	57	18 ± 2	−150 ± 6
$[Co(bpy)_2]^{2+}$	$[Co(ox)_3]^{3-}$	160 ± 20			
$[Co(4,7\text{-}Me_2phen)_3]^{2+}$	$[Co(ox)_3]^{3-}$	523 ± 25	850		
$[Co(5,6\text{-}Me_2phen)_3]^{2+}$	$[Co(ox)_3]^{3-}$	~250	400		
$[Co(phen)_3]^{2+}$	$[Co(phen)_2(ox)]^+$	3.5 ± 0.7			
$[Co(bpy)_3]^{2+}$	$[Co(bpy)_2(ox)]^+$	1.6 ± 0.5			

[a] Radii used were as follows: $[Co(ox)_3]^{3-}$, 5 Å; $[Co(bpy)_3]^{2+}$, 6 Å; $[Co(phen)_3]^{2+}$, 7 Å; $[Co(4,7\text{-}Me_2phen)_3]^{2+}$, 8 Å; $[Co(5,6\text{-}Me_2phen)_3]^{2+}$, 8 Å.

reduction by $[Co(phen)_2]^{2+}$. An extensive $[Co(phen)_2]^{2+}$ concentration dependence is not possible due to uncertainties in the distribution of different forms of the reductant.

In the corresponding reductions by $[Co(bpy)_3]^{2+}$ and $[Co(4,7\text{-}Me_2phen)_3]^{2+}$, limiting first-order behavior is also observed with $k_{os} = 50 \pm 2\ M^{-1}\ s^{-1}$, $K_0 = 56 \pm 20\ M^{-1}$, $k_{et} = 0.89 \pm 0.32\ s^{-1}$, and $k_{os} = 523 \pm 25\ M^{-1}\ s^{-1}$, $K_0 = 200 \pm 60\ M^{-1}$, $k_{et} = 2.6 \pm 0.8\ s^{-1}$, respectively. No concentration dependence was carried out with $[Co(5,6\text{-}Me_2phen)_3]^{2+}$, since this species readily forms precipitates in the presence of $[Co(ox)_3]^{3-}$. An estimate for $k_{os} \approx 250\ M^{-1}\ s^{-1}$ is based on reaction half-lives. The second-order rate for reduction by $[Co(bpy)_3]^{2+}$ shows a dependence on [bpy] analogous to that given by eq 5 with $k_{os} = 49 \pm 2\ M^{-1}\ s^{-1}$ and $k_{is} = 160 \pm 20\ M^{-1}\ s^{-1}$. Data at lower [4,7-$Me_2$phen] concentrations where $[Co(4,7\text{-}Me_2phen)_2]^{2+}$ predominates could not be obtained because of problems encountered with rapid precipitation. Second-order rate constants for all the reactions are summarized in Table III.

(c) **Stereoselectivity.** The circular dichroism response at 487 nm for the reaction of $\Delta\text{-}(+)_{589}\text{-}[Co(ox)_3]^{3-}$ with an excess of $[Co(phen)_3]^{2+}$ at 25.0 °C in 0.017 M KNO_3 media is shown in Figure 3. Since $\Delta\text{-}(+)_{589}\text{-}[Co(ox)_3]^{3-}$ has a very small signal at this wavelength, the signal represents almost exclusively the formation of optically active $[Co(phen)_3]^{3+}$.[41] The signal reaches a maximum and then slowly decays to the baseline, the result of racemization of $[Co(phen)_3]^{3+}$ by electron self-exchange in the presence of $[Co(phen)_3]^{2+}$. The reaction trace was fit according to eq 6, where l is the pathlength, k_{so} is the known rate of the

$$\frac{\phi}{3300l} = \left\{\Delta\epsilon_{ox}\exp(-k_{so}[Co(II)]t) + \Delta\epsilon_{app}\frac{k_{so}}{k_{ex} - k_{so}}\{\exp(-k_{so}[Co(II)]t) - \exp(-k_{ex}[Co(II)]t)\}\right\}[[Co(ox)_3]^{3-}] \quad (6)$$

primary electron-transfer reaction, in this case the formation of $[Co(phen)_3]^{3+}$, k_{ex} is the rate of racemization of the immediate reaction product, which in this instance is the self-exchange rate of $[Co(phen)_3]^{3+/2+}$, $\Delta\epsilon_{ox}$ is $\Delta\epsilon$ for $[Co(ox)_3]^{3-}$ at this wavelength, and $\Delta\epsilon_{app}$ is the apparent $\Delta\epsilon$ for the product at this wavelength. The stereoselectivity is $\Delta\epsilon_{app}/\Delta\epsilon$, the apparent optical purity (enantiomeric excess) of the product. Rate constants k_{so}, k_{ex} and stereoselectivities are presented in Table IV for this reaction and for the reactions of the other reductants under a variety of conditions. The induction in the reaction with $[Co(phen)_3]^{2+}$ is 24 ± 1% ΔΔ[42] at ionic strength 0.017 M and 25.0 °C and is relatively insensitive to the ionic medium. It is also relatively insensitive to $[[Co(phen)_3]^{2+}]$ over the range 3×10^{-4}–6×10^{-3} M. Derived rate constants are in good agreement with those obtained independently for k_{so} ($=k_{os}$) and for k_{ex}. No effect of ionic strength was observed over the range 0.01–0.04 M. Addition of sufficient 18-crown-6 to complex out ≥90% of the K^+ or addition of sufficient [2.2.2] cryptand to complex out ≥99% of the K^+ likewise has no effect on the stereoselectivity, although there does appear to be a slight reduction in the stereoselectivity at higher pH.

The stereoselectivities for $[Co(phen)_3]^{2+}$ and $[Co(bpy)_3]^{2+}$ were obtained over a temperature range 5.0–45.0 °C. For $[Co(bpy)_3]^{2+}$ where the stereoselectivity is small, the effect of temperature is within the experimental error. For $[Co(phen)_3]^{2+}$, there is a reduction in the stereoselectivity from 28% ΔΔ to 20% ΔΔ as the temperature is increased from 5.0 to 45.0 °C. This yields values

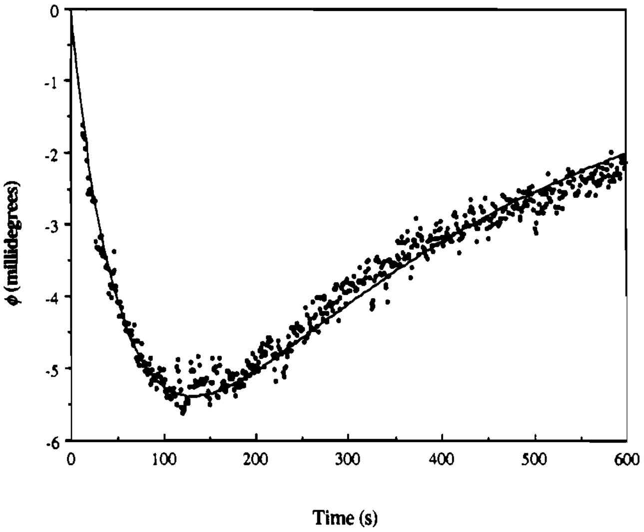

Figure 3. Circular dichroism response at 487 nm for the reaction of 1.10×10^{-4} M $\Delta\text{-}(+)_{589}\text{-}[Co(ox)_3]^{3-}$ with 1.13×10^{-3} M $[Co(phen)_3]^{2+}$ (pH = 7.0 (TRIS buffer), 0.017 M ionic strength (KNO_3), 25.0 °C).

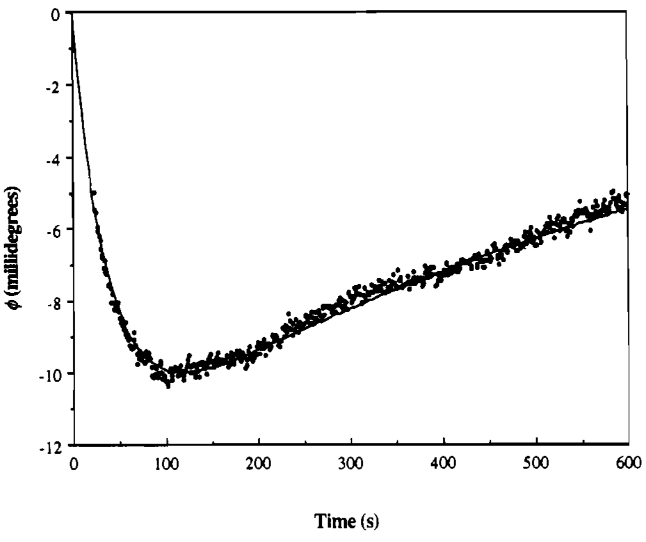

Figure 4. Circular dichroism response at 520 nm for the reaction of 1.10×10^{-4} M $\Delta\text{-}(+)_{589}\text{-}[Co(ox)_3]^{3-}$ with 1.13×10^{-3} M $[Co(phen)_2]^{2+}$ (pH = 7.0 (TRIS buffer), 0.017 M ionic strength (KNO_3), 25.0 °C).

---

(41) The signal is absent when the process is monitored at 435 nm, where $[Co(phen)_3]^{3+}$ has a negligible circular dichroism signal.

(42) This refers to 24% optical purity (enantiomeric excess) in the product $\Delta\text{-}[Co(phen)_3]^{3+}$ obtained from $\Delta\text{-}[Co(ox)_3]^{3-}$.

Table IV. Stereoselectivities for the Reduction of $[\Delta\text{-}(+)_{589}\text{-Co(ox)}_3]^{3-}$ with $[\text{Co(phen)}_3]^{2+}$, $[\text{Co(phen)}_2]^{2+}$, and Derivatives[a]

reductant	temp, °C	[Co(II)], 10^3 M	*I*, M	k_{so}, $M^{-1}\,s^{-1}$	k_{ex}, $M^{-1}\,s^{-1}$	stereoselectivity (ee)
$[\text{Co(phen)}_3]^{2+}$	5.0	1.13	0.017	6.8	1.3	28 ± 1% ΔΔ
$[\text{Co(phen)}_3]^{2+}$	5.0	5.37	0.017	6.6	0.7	28 ± 1% ΔΔ[b]
$[\text{Co(phen)}_3]^{2+}$	25.0	0.27	0.011	18.6	4	24 ± 1% ΔΔ
$[\text{Co(phen)}_3]^{2+}$	25.0	1.10	0.014	16	2	24 ± 1% ΔΔ
$[\text{Co(phen)}_3]^{2+}$	25.0	1.10	0.014	16	2	24 [illegible] 2% ΔΔ[d]
$[\text{Co(phen)}_3]^{2+}$	25.0	1.10	0.014	16	2	23 ± 2% ΔΔ[e]
$[\text{Co(phen)}_3]^{2+}$	25.0	1.13	0.017	15.8	2.3	24 ± 1% ΔΔ
$[\text{Co(phen)}_3]^{2+}$	25.0	1.08	0.017	15.8	2.3	23 ± 1% ΛΛ[f]
$[\text{Co(phen)}_3]^{2+}$	25.0	1.10	0.017	15.8	2.5	21 ± 1% ΔΔ[c]
$[\text{Co(phen)}_3]^{2+}$	25.0	1.10	0.017	15.8	3	21 ± 1% ΔΔ[c,g]
$[\text{Co(phen)}_3]^{2+}$	25.0	1.79	0.017	14	2.4	26 ± 2% ΔΔ[b]
$[\text{Co(phen)}_3]^{2+}$	25.0	2.19	0.017	15.8	1.8	25 ± 1% ΔΔ
$[\text{Co(phen)}_3]^{2+}$	25.0	4.30	0.017	12	1.9	27 ± 2% ΔΔ[b]
$[\text{Co(phen)}_3]^{2+}$	25.0	5.37	0.017	11	1.7	27 ± 2% ΔΔ[b]
$[\text{Co(phen)}_3]^{2+}$	25.0	1.10	0.026	11.7	3	24 ± 1% ΔΔ
$[\text{Co(phen)}_3]^{2+}$	25.0	1.10	0.039	7	4.5	26 ± 2% ΔΔ
$[\text{Co(phen)}_3]^{2+}$	45.0	1.13	0.017	33	5	20 ± 1% ΔΔ
$[\text{Co(phen)}_3]^{2+}$	45.0	5.37	0.017	20	3	21 ± 2% ΔΔ[b]
$[\text{Co(bpy)}_3]^{2+}$	5.0	1.10	0.017	35	1	3 ± 2% ΔΔ
$[\text{Co(bpy)}_3]^{2+}$	25.0	1.10	0.017	43	4	5 ± 2% ΔΔ
$[\text{Co(4,7-Me}_2\text{phen)}_3]^{2+}$	25.0	1.10	0.017	550[h]	24	43 ± 2% ΔΔ
$[\text{Co(5,6-Me}_2\text{phen)}_3]^{2+}$	25.0	1.10	0.017	250[h]	56	19 ± 2% ΔΔ
$[\text{Co(bpy)}_2]^{2+}$	25.0	1.10	0.017	93	3.5	19 ± 3% ΔΔ[j]
$[\text{Co(phen)}_2]^{2+}$	25.0	0.56	0.017	23.4	0.8	63 ± 5% ΔΔ[k]
$[\text{Co(phen)}_2]^{2+}$	25.0	1.13	0.017	23.4	1.2	59 ± 5% ΔΔ[k]
$[\text{Co(phen)}_2]^{2+}$	25.0	2.25	0.017	23.4	1.4	51 ± 5% ΔΔ[k]

[a] pH 7.0, 0.01 M TRIS, KNO_3 media. [b] pH 8.0, 0.001 M TRIS, KNO_3 media. [c] pH 10.4, 0.01 M CAPS, KNO_3 media. [d] With sufficient 18-crown-6 to complex out >79% of K^+. [e] With sufficient 18-crown-6 to complex out >88% of K^+. [f] Oxidation using $[\Lambda\text{-}(-)_{589}\text{-Co(ox)}_3]^{3-}$. [g] With sufficient cryptand-222 to complex out >99% of K^+. [h] Too rapid for detection on the CD instrument; value quoted was obtained from conventional stopped-flow studies. [j] Corrected for the fact that only 88% of the immediate reaction product is $[\text{Co(bpy)}_2\text{(ox)}]^+$. [k] Corrected for the fact that only 91% of the immediate reaction product is $[\text{Co(phen)}_2\text{(ox)}]^+$.

for $\Delta\Delta H^{\ddagger}(\Delta\Delta\text{–}\Delta\Lambda) = -3.1 \pm 0.5$ kJ mol^{-1} and $\Delta\Delta S^{\ddagger}(\Delta\Delta\text{–}\Delta\Lambda) = -6.4 \pm 1.5$ J K^{-1} mol^{-1} at 25.0 °C.[43]

In the reaction with $[\text{Co(phen)}_3]^{2+}$ at lower [phen] concentrations where $[\text{Co(phen)}_2]^{2+}$ predominates, the circular dichroism response of the reaction is markedly different (Figure 4). Approximately 10% of the immediate reaction product is identified as $[\text{Co(phen)}_3]^{3+}$ and shows a circular dichroism response similar to that observed at higher [phen] concentrations. The bulk of the immediate reaction product, ≈90%, is $[\text{Co(phen)}_2\text{(ox)}]^+$, which has a circular dichroism peak at 520 nm. This latter species also undergoes racemization in the presence of an excess of $[\text{Co(phen)}_2]^{2+}$, and the stereoselectivity was again evaluated with use of eq 6. The behavior of $[\text{Co(bpy)}_2]^{2+}$ is similar, and the results for both reductants at 25.0 °C in 0.017 M KNO_3 media are also shown in Table IV.

(d) Racemization of $[\text{Co(bpy)}_3]^{3+}$ by $[\text{Co(bpy)}_3]^{2+}$. The racemization of $[\text{Co(phen)}_3]^{3+}$ in the presence of $[\text{Co(phen)}_3]^{2+}$ has been shown previously to be dominated by the self-exchange reaction, and rates have been reported for the $[\text{Co(phen)}_3]^{3+/2+}$, $[\text{Co(4,7-Me}_2\text{phen)}_3]^{3+/2+}$, and $[\text{Co(5,6-Me}_2\text{phen)}_3]^{3+/2+}$ systems.[15] Similar measurements are now reported for the $[\text{Co(bpy)}_3]^{3+/2+}$ system.

At 25.0 °C and in 0.10 M nitrate media, the rate law for racemization of $[\text{Co(bpy)}_3]^{3+}$ in the presence of $[\text{Co(bpy)}_3]^{2+}$ is given by eq 7, where $k_a = (2 \pm 2) \times 10^{-4}$ s^{-1} and $k_b = 5.7 \pm 0.2$

$$-d\phi/dt = \{k_a + k_b[\text{Co(II)}]\}\phi \qquad (7)$$

M^{-1} s^{-1} (Figure 5). The value for k_a is zero within experimental error and consistent with a half-life in excess of 60 h obtained for the racemization of $\Delta\text{-}(-)_{589}\text{-}[\text{Co(bpy)}_3]^{3+}$ in the absence of added $[\text{Co(bpy)}_3]^{2+}$. The value obtained for k_b is related directly to the self-exchange rate of $[\text{Co(bpy)}_3]^{3+/2+}$ (eq 8) provided the

$$\Delta\text{-}(-)_{589}\text{-}[\text{Co(bpy)}_3]^{3+} + rac\text{-}[\text{Co(bpy)}_3]^{2+} \xrightarrow{k_{ex}} rac\text{-}[\text{Co(bpy)}_3]^{3+} + \Delta\text{-}[\text{Co(bpy)}_3]^{2+} \qquad (8)$$

$$\Delta\text{-}[\text{Co(bpy)}_3]^{2+} \xrightarrow{k_{inv3}} \Lambda\text{-}[\text{Co(bpy)}_3]^{2+} \qquad (9)$$

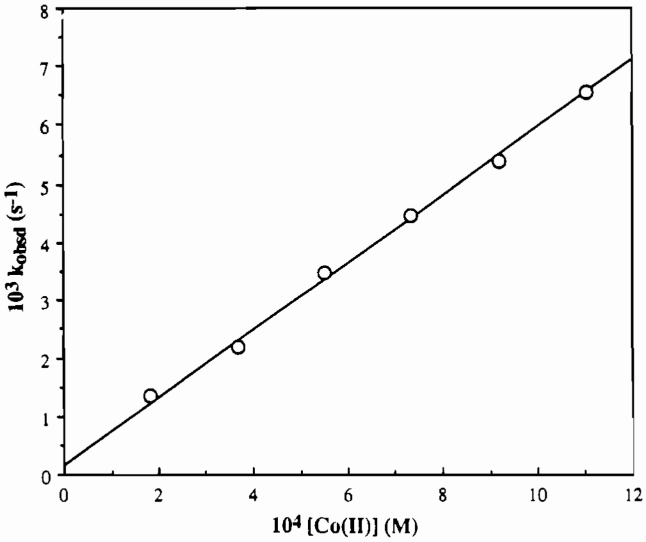

Figure 5. Plot of observed pseudo-first-order rate constant, k_{obsd}, against $[\text{Co(bpy)}_3]^{2+}$ concentration for the reduction of $\Delta\text{-}(-)_{589}\text{-}[\text{Co(bpy)}_3]^{3+}$ by $[\text{Co(bpy)}_3]^{2+}$ (pH = 7.0 (TRIS buffer), 0.10 M ionic strength ($NaNO_3$), 25.0 °C).

rate of inversion, k_{inv3} of eq 9, of the labile $[\text{Co(bpy)}_3]^{2+}$ exceeds the rate of the electron-transfer reaction and also provided that the electron transfer shows no significant chiral discrimination. It is assumed that both of these conditions are met for the $[\text{Co(bpy)}_3]^{3+/2+}$ system as they are for $[\text{Co(phen)}_3]^{3+/2+}$.[15] The rate of the self-exchange reaction was determined to be 5.7 ± 0.2 M^{-1} s^{-1} in 0.10 M nitrate media and 1.7 ± 0.2 M^{-1} s^{-1} in 0.017 M nitrate media, both at 25.0 °C. Activation parameters determined over the range 5–45 °C yield $\Delta H^{\ddagger} = 31.1 \pm 0.6$ kJ mol^{-1} and $\Delta S^{\ddagger} = -127 \pm 2$ J K^{-1} mol^{-1} at 25.0 °C in 0.10 M nitrate media. Previously a rate constant of 20 M^{-1} s^{-1} was quoted for this reaction[44] with $\Delta H^{\ddagger} = 32$ kJ mol^{-1} and $\Delta S^{\ddagger} = -133$ J K^{-1} mol^{-1}

---

(43) $\Delta\Delta H^{\ddagger}(\Delta\Delta\text{–}\Delta\Lambda) = \Delta H^{\ddagger}_{\Delta\Delta} - \Delta H^{\ddagger}_{\Delta\Lambda}$, $\Delta\Delta S^{\ddagger}(\Delta\Delta\text{–}\Delta\Lambda) = \Delta S^{\ddagger}_{\Delta\Delta} - \Delta S^{\ddagger}_{\Delta\Lambda}$.

(44) Endicott, J. F.; Kumar, K.; Ramasami, T.; Rotzinger, F. P. *Prog. Inorg. Chem.* **1983**, *30*, 151.

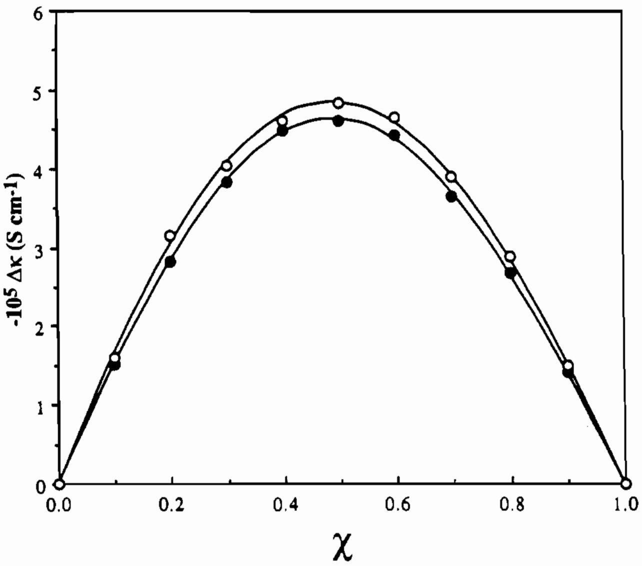

Figure 6. Deviations, $\Delta\kappa$, of the observed conductivity from additivity as a function of the volume fraction of the ruthenium complex, χ, for the ΔΔ (white circles) and ΔΛ (black circles) $[Ru(phen)_3]^{2+}/[Rh(ox)_3]^{3-}$ ion pairs at 25.00 °C and 0.01 M ionic strength.

in 0.10 M nitrate media[45] in reasonable agreement with the results of the present study.

(e) Racemization of $[Co(phen)_2(ox)]^+$ by $[Co(phen)_2]^{2+}$ and of $[Co(bpy)_2(ox)]^+$ by $[Co(bpy)_2]^{2+}$. In the case of reactions carried out at lower [phen] concentrations, the immediate product is $[Co(phen)_2(ox)]^+$. Racemization of the $[Co(phen)_2(ox)]^+$ in the presence of an excess of $[Co(phen)_2]^{2+}$ could occur by either a pseudo-self-exchange inner-sphere process (eqs 10 and 11) or by

$$\Delta\text{-}[Co(phen)_2(ox)]^+ + rac\text{-}[Co(phen)_2]^{2+} \rightarrow rac\text{-}[Co(phen)_2(ox)]^+ + \Delta\text{-}[Co(phen)_2]^{2+} \quad (10)$$

$$\Delta\text{-}[Co(phen)_2]^{2+} \xrightarrow{k_{inv2}} \Lambda\text{-}[Co(phen)_2]^{2+} \quad (11)$$

outer-sphere oxidation of the $[Co(phen)_3]^{2+}$ present in the reaction mixture by $[Co(phen)_2(ox)]^+$. The rate of this latter reaction was measured independently as 3.5 ± 0.7 M^{-1} s^{-1} at 25.0 °C and 0.017 M ionic strength. Under the conditions of the racemization reaction, only 28% of the cobalt(II) is present as $[Co(phen)_3]^{2+}$ and hence the apparent second-order rate constant expected for this pathway is ≈1 M^{-1} s^{-1}, close to the value of 1.2 ± 0.2 M^{-1} s^{-1} which is obtained from the data analysis. The rate constant for the corresponding reduction of $[Co(bpy)_2(ox)]^+$ by $[Co(bpy)_3]^{2+}$ is 1.6 ± 0.5 M^{-1} s^{-1} under the same conditions, and in this instance only 26% of the cobalt(II) is present as $[Co(bpy)_3]^{2+}$. Thus the rate expected for the racemization by reduction with $[Co(bpy)_3]^{2+}$ is 0.4 M^{-1} s^{-1}, 1 order of magnitude smaller than the rate observed which is consequently ascribed to a predominant pseudo-self-exchange process (eqs 10 and 11).

(f) Conductivity. Investigation of thermodynamic aspects of chiral recognition between $[Co(ox)_3]^{3-}$ and $[Co(phen)_3]^{2+}$ by conductivity experiments is not possible because of the electron-transfer reactivity of the system. However, redox inactive ions of similar structure and charge can be used to obtain information on the interactions. The ions chosen, $[Rh(ox)_3]^{3-}$ and $[Ru(phen)_3]^{2+}$, are readily resolved and purified and do not racemize in aqueous solution to any appreciable extent over the time scale required for the conductivity experiments.

Diastereomeric ion-pair formation constants were determined by the method of Katayama and Tamamushi.[46] The observed conductivities κ of the mixed solutions of $[Ru(phen)_3]^{2+}$ and $[Rh(ox)_3]^{3-}$ as a function of the volume fraction χ of the ruthenium salt solution were measured for ΔΔ and ΔΛ pairs at 25.00 °C and 0.01 M ionic strength. Deviations from additivity ($\Delta\kappa$) of the conductivity measured for a mixture of the pure components are observed (Figure 6). These deviations are described by eq 12,

$$1000\Delta\kappa = 1000\kappa - [K_3[Rh(ox)_3]](1 - \chi)\Lambda_m(Rh) - [[Ru(phen)_3]Br_2]\chi\Lambda_m(Ru) \quad (12)$$

where κ is the specific conductivity of the mixture, $\Lambda_m(Ru)$ is the molar conductivity for $[Ru(phen)_3]Br_2$, and $\Lambda_m(Rh)$ is the molar conductivity for $K_3[Rh(ox)_3]$ at ionic strength 0.01 M. If the deviation is due solely to 1:1 ion-pair formation between $[Ru(phen)_3]^{2+}$ and $[Rh(ox)_3]^{3-}$, then the concentration of the ion pair $\{[Ru(phen)_3],[Rh(ox)_3]\}^-$ is given by eq 13, where λ_{RuRh} is the

$$[\{[Ru(phen)_3],[Rh(ox)_3]\}^-] = \frac{1000\Delta\kappa}{\lambda_{RuRh} - 3\lambda_{Rh} - 2\lambda_{Ru}} \quad (13)$$

equivalent conductance of the ion pair, λ_{Ru} is the equivalent conductance of $[Ru(phen)_3]^{2+}$, and λ_{Rh} is the equivalent conductance of $[Rh(ox)_3]^{3-}$, all at ionic strength 0.01 M. The values of λ at this ionic strength were estimated by the use of the corresponding transport numbers[47] calculated from their limiting equivalent conductivities λ_0 given in Table II, and λ_{RuRh} was approximated to be $\lambda_{Rh}/3$. In the calculation of the ion-pair formation constants K_0, it was necessary to take into account the changes in the ionic strength due to ion-pair formation. For example, in the solution of $\chi = 0.5$ at 0.01 M ionic strength, the ionic strength decreased by about 12%. Values of K_0 at 0.01 M ionic strength were obtained by correcting the apparent values at the ionic strength for each fraction with use of activity coefficients evaluated from the Guggenheim–Davies equation.[48] A summary of the diastereomeric ion pair formation constants and the discrimination factors at 25 °C and $I = 0.01$ M for the ΔΔ and ΔΛ pairs as well as the ΛΛ and ΛΔ pairs is presented in Table V. There is a small, 5%, discrimination favoring the homochiral (ΔΔ or ΛΛ) pairs over the heterochiral (ΛΔ or ΔΛ) pair. At the higher ionic strengths used for the kinetic studies, a less extensive examination was carried out.[49] A good estimate of the chiral recognition in the system is possible by examining the ratio $\Delta\kappa(\Delta\Delta)/\Delta\kappa(\Delta\Lambda)$, which is directly related to $K_0(\Delta\Delta)/K_0(\Delta\Lambda)$ when the extent of ion-pair formation is small. At 25.0 °C, the ratio is 1.006 ± 0.027, showing almost no discrimination, while, at 45.0 °C, the ratio is 0.977 ± 0.027 with a small preference, ≈1%, for the heterochiral ion pair. At lower temperatures, problems with precipitation were encountered, especially for the homochiral pair, and no data are reported below 25.0 °C. These ratios allow the estimation of thermodynamic parameters associated with the chiral recognition, $\Delta\Delta H°(\Delta\Delta-\Delta\Lambda) = -1.3 \pm 1.1$ kJ mol^{-1} and $\Delta\Delta S°(\Delta\Delta-\Delta\Lambda) = -4.3 \pm 3.5$ J K^{-1} mol^{-1}.

(g) Chromatographic Observation of Favorable Ion Pairs. In Figure 7 is shown the elution curves and percentage resolutions

Table V. Summary of Ion-Pair Formation Constants and Discrimination Factors for the Diastereomeric Pairs between $[Ru(phen)_3]^{2+}$ and $[Rh(ox)_3]^{3-}$ at 25.00 °C and 0.01 M Ionic Strength

diastereomeric pair	ion-pair formation constant, M^{-1}	discrimination factor
ΛΛ	205 ± 7	
ΛΔ	193 ± 6	1.06 ± 0.02
ΔΛ	196 ± 6	
ΔΔ	206 ± 7	1.05 ± 0.02

---

(45) H. M. Neumann, as quoted in: Farina, R.; Wilkins, R. G. *Inorg. Chem.* **1968**, *7*, 514–518.

(46) Katayama, S.; Tamamushi, R. *Bull. Chem. Soc. Jpn.* **1970**, *43*, 2354–2359.

(47) Robinson, R. A.; Stokes, R. H. *Electrolyte Solutions*, 2nd ed.; Butterworths: London, 1959; p 156.

(48) Davies, C. W. *J. Chem. Soc.* **1938**, 2093–2098.

(49) At higher ionic strength (and higher concentrations), the conductivity data are more prone to systematic deviations due to competing equilibria. For example, ion multiplet formation occurs in solutions of $[Ru(phen)_3]^{2+}$. However, estimates of the ion-pairing constant can be obtained by the method outlined in the text to give $K_0(25\ °C) = 157 \pm 7$ M^{-1} and $K_0(45\ °C) = 133 \pm 7$ M^{-1}, from which $\Delta H° \approx -6.5$ kJ mol^{-1} and $\Delta S° \approx 20$ J K^{-1} mol^{-1} at 0.017 M ionic strength.

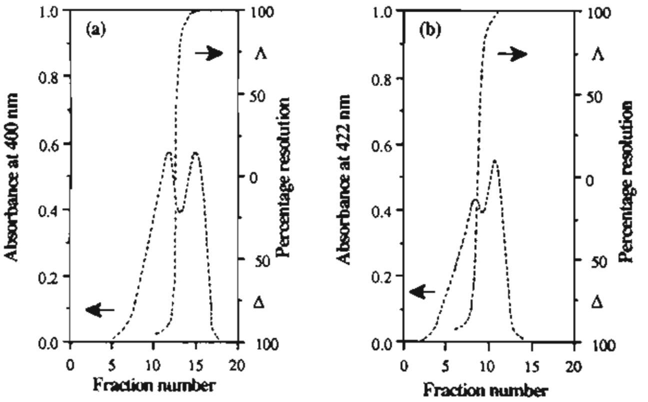

Figure 7. Elution curves and percentage resolutions for $[\mathrm{Rh(ox)_3}]^{3-}$ and $[\mathrm{Co(ox)_3}]^{3-}$ eluted with water down an SP-Sephadex C-25 ion-exchange resin saturated with Λ-(+)$_{589}$-$[\mathrm{Ru(phen)_3}]^{2+}$: (a) 0.5- × 20-cm column, $[\mathrm{Rh(ox)_3}]^{3-}$; (b) 0.5- × 16-cm column, $[\mathrm{Co(ox)_3}]^{3-}$.

of $[\mathrm{Rh(ox)_3}]^{3-}$ and $[\mathrm{Co(ox)_3}]^{3-}$ in chromatography where a column of SP-Sephadex ion-exchanger in the Δ-$[\mathrm{Ru(phen)_3}]^{2+}$ form and water as an eluent were employed at ambient temperature (17 ± 3 °C). It can be expected that the enantiomer which interacts favorably with Λ-$[\mathrm{Ru(phen)_3}]^{2+}$ in the resin is eluted more slowly in this type of chromatography. The Λ enantiomers of $[\mathrm{Rh(ox)_3}]^{3-}$ and $[\mathrm{Co(ox)_3}]^{3-}$ elute more slowly, indicating that the ΛΛ pair is more favorable than the ΛΔ pair.

(h) NMR Ion-Pair Structure. Consideration of the thermodynamics of ion-pair formation prompts a number of questions regarding structure in the ion pairs. In previous work,[50] ^{1}H relaxation experiments in the presence of paramagnetic ions provided valuable information on the structures of labile ion pairs. To facilitate the investigation, the complex $[\mathrm{Co(phen)_3}]^{3+}$ was used as a diamagnetic isostructural analogue for $[\mathrm{Co(phen)_3}]^{2+}$ and the interaction of this complex with $[\mathrm{Cr(ox)_3}]^{3-}$, a paramagnetic analogue for $[\mathrm{Co(ox)_3}]^{3-}$, was investigated. Four ^{1}H environments are readily distinguished in the spectrum of $[\mathrm{Co(phen)_3}]^{3+}$, and the assignments are shown in Table VI.

In a structured ion pair with the paramagnetic ion, $[\mathrm{Cr(ox)_3}]^{3-}$, the ^{1}H NMR relaxation times (T_1) for $[\mathrm{Co(phen)_3}]^{3+}$ decrease according to eq 14, where $M_{\rm diam}$ is the mole fraction of $[\mathrm{Co(phen)_3}]^{3+}$ free in solution, $M_{\rm para}$ is the mole fraction in the structured ion pair, $(1/T_1)_{\rm diam}$ is the relaxation rate in the absence of the paramagnetic ion, and $(1/T_1)_{\rm para}$ is the relaxation rate in the isolated structured ion pair. When the diamagnetic complex is present in large excess, eq 14 can be modified to eq 15, where

$$(1/T_1)_{\rm obsd} = M_{\rm diam}(1/T_1)_{\rm diam} + M_{\rm para}(1/T_1)_{\rm para} \quad (14)$$

$$(1/T_1)_{\rm obsd} = (1/T_1)_{\rm diam} + \frac{K_0}{1 + K_0[\mathrm{Co(III)}]_T}(1/T_1)_{\rm para}[[\mathrm{Cr(ox)_3}]^{3-}] \quad (15)$$

the term $(\{K_0/(1 + K_0[\mathrm{Co(III)}]_T)\}(1/T_1)_{\rm para}) = R_{\rm struct}$ is defined as the relaxivity due to the structured ion pair. Additional contributions to the relaxivities from unstructured interactions, $R_{\rm unstruct}$, will also occur, and these will also show a linear dependence on $[[\mathrm{Cr(ox)_3}]^{3-}]$.[50] The dependencies of $(1/T_1)_{\rm obsd}$ on $[[\mathrm{Cr(ox)_3}]^{3-}]$ for the four ^{1}H environments in $[\mathrm{Co(phen)_3}]^{3+}$ are indeed linear and vary with the position of the ^{1}H on the ligand backbone (Table VI), a characteristic of well-structured ion-pairing interactions. $R_{\rm struct}$ and $R_{\rm unstruct}$ can be separated by least-squares optimization of the Solomon–Bloembergen[51,52] correlation between $R_{\rm struct}$ and $(1/N)\sum(1/r_i^6)$, where r_i is the distance between the paramagnetic center and the ith equivalent proton and N is the number of equivalent proton environments in the complex. Thus, the position of the paramagnetic center relative to the protons can be calculated as shown in Figure 8. For data at 0.1 M ionic strength the paramagnetic center is close to the C_3 axis of $[\mathrm{Co(phen)_3}]^{3+}$, with a Co–Cr distance of 5.9 Å. A value for $K_0 \approx 30$ M^{-1} can be estimated by assigning a correlation time for the ion pair of 1.2 × 10^{-10} s.[53] The component of the relaxivity which shows no correlation with distance is assigned to the unstructured or random interactions and is substantial, amounting to 8 × 10^4 s^{-1}, from which it can be estimated that the structured ion pair contributes no more than 30% to all ion-pair structures.[54] A similar result is obtained at 0.017 M ionic strength with $K_0 \approx 100$ M^{-1}.

Table VI. Relaxation Rates ($1/T_1$) and Slopes (Relaxivities) from Plots of ($1/T_1$) against $[[\mathrm{Cr(ox)_3}]^{3-}]$ for the Protons in $[\mathrm{Co(phen)_3}]^{3+}$ at 25 °C

Ionic Strength = 0.10 M			(1/T$_1$) (s^{-1})				10^{-4} Relaxivity (M^{-1} s^{-1})
10^4 [[Cr(ox)$_3$]$^{3-}$] (M)	0.00	1.49	2.98	4.97	6.95	9.93	
2,9 (7.6 ppm, d)	1.0	27	65				21.4 ± 2.4
3,8 (7.9 ppm, dd)	1.0	27	62				20.4 ± 1.8
4,7 (9.0 ppm, d)	0.9	16	31	47	69		9.6 ± 0.3
5,6 (8.4 ppm, s)	0.9	14	33	41	54	88	8.3 ± 0.6

Ionic Strength = 0.017 M		(1/T$_1$) (s^{-1})			10^{-4} Relaxivity (M^{-1} s^{-1})
10^4 [[Cr(ox)$_3$]$^{3-}$] (M)	0.00	0.37	0.93	1.48	
2,9 (7.6 ppm, d)	1.0	41	85	147	97.0 ± 2.3
3,8 (7.9 ppm, dd)	1.0	30	80	114	78.8 ± 1.4
4,7 (9.0 ppm, d)	0.9	18	29	57	35.9 ± 2.1
5,6 (8.4 ppm, s)	0.9	14	37	58	38.5 ± 0.4

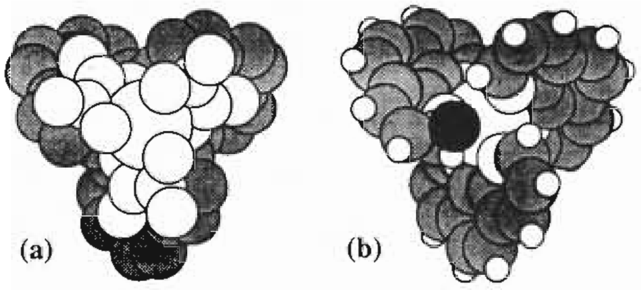

Figure 8. (a) Representation along the C_3 axis of the interaction of Δ-(+)$_{589}$-$[\mathrm{Co(ox)_3}]^{3-}$ with Δ-(−)$_{589}$-$[\mathrm{Ni(phen)_3}]^{2+}$ in the crystal structure of K(Δ-(−)$_{589}$-[Ni(phen)$_3$])(Δ-(+)$_{589}$-[Co(ox)$_3$])·2H$_2$O.[29] (b) Representation along the C_3 axis of the position of the paramagnetic center with a $[\mathrm{Co(phen)_3}]^{3+}$ ion derived from correlation of Cr–^{1}H distances with NMR relaxation rates (T_1).

Discussion

The reduction of $[\mathrm{Co(ox)_3}]^{3-}$ by $[\mathrm{Co(phen)_3}]^{2+}$ takes place by two parallel pathways, an outer-sphere pathway (eq 16), leading to the direct formation of $[\mathrm{Co(phen)_3}]^{3+}$, and an inner-sphere pathway (eq 17), where the immediate reaction product, $[\mathrm{Co(phen)_2(ox)}]^{+}$, is formed by transfer of a doubly bridged oxalate

$$[\mathrm{Co(ox)_3}]^{3-} + [\mathrm{Co(phen)_3}]^{2+} \rightarrow [\mathrm{Co(phen)_3}]^{3+} + [\mathrm{Co(ox)_2}]^{2-} + \mathrm{ox}^{2-} \quad (16)$$

$$[\mathrm{Co(ox)_3}]^{3-} + [\mathrm{Co(phen)_2}]^{2+} \rightarrow [\mathrm{Co(phen)_2(ox)}]^{+} + [\mathrm{Co(ox)_2}]^{2-} \quad (17)$$

$$[\mathrm{Co(phen)_2(ox)}]^{+} + [\mathrm{Co(phen)_3}]^{2+} \rightarrow [\mathrm{Co(phen)_3}]^{3+} + [\mathrm{Co(phen)_2(ox)}] \quad (18)$$

---

(50) Marusak, R. A.; Lappin, A. G. *J. Phys. Chem.* **1989**, *93*, 6856–6859.

(51) Solomon, I. *Phys. Rev.* **1955**, *99*, 559–565.

(52) Bloembergen, N. *J. Chem. Phys.* **1957**, *27*, 572–573.

(53) Masuda, Y.; Yamatera, H. *J. Phys. Chem.* **1984**, *88*, 3425–3431.

(54) Some idea of the relative proportions of the structured and unstructured components can be obtained by treating the $[\mathrm{Cr(ox)_3}]^{3-}$ and $[\mathrm{Co(phen)_3}]^{3+}$ as spheres with radii 4.25 and 6.25 Å, respectively. The average Co–^{1}H distance in $[\mathrm{Co(phen)_3}]^{3+}$ is then ≈5 Å from Co, or ≈5.5 Å from the paramagnetic center in the unstructured pair. The $1/T_1$ value for the unstructured component is approximately 3 times the value calculated for a Cr–^{1}H distance of 5.5 Å in the structured ion pair. Longer range interactions are ignored but may also be significant.

group from $[\mathrm{Co(ox)_3}]^{3-}$ to $[\mathrm{Co(phen)_2}]^{2+}$. Subsequent reduction of the $[\mathrm{Co(phen)_2(ox)}]^{+}$ by $[\mathrm{Co(phen)_3}]^{2+}$ (eq 18) results in $[\mathrm{Co(phen)_3}]^{3+}$ as the thermodynamic product from both pathways. A similar mechanism is noted in the corresponding reduction of $[\mathrm{Co(ox)_3}]^{3-}$ by $[\mathrm{Co(bpy)_3}]^{2+}$ and by $[\mathrm{Co(en)_3}]^{2+}$, where en = 1,2-diaminoethane.[7]

The inner-sphere reaction of $[\mathrm{Co(ox)_3}]^{3-}$ with $[\mathrm{Co(phen)_2}]^{2+}$ has a second-order rate constant of 94 $\mathrm{M^{-1}\,s^{-1}}$, faster than the corresponding outer-sphere reaction involving $[\mathrm{Co(phen)_3}]^{2+}$ despite a thermodynamic disadvantage. There is clearly a considerable kinetic advantage in the inner-sphere pathway. The rate-limiting step is likely to be electron transfer as the second-order rate constants are much slower than the rates of substitution at a cobalt(II) center. Corresponding rates for reduction by $[\mathrm{Co(bpy)_2}]^{2+}$ and $[\mathrm{Co(en)_2}]^{2+}$ are respectively 160 $\mathrm{M^{-1}\,s^{-1}}$ and 3300 $\mathrm{M^{-1}\,s^{-1}}$,[7] showing a trend with the expected driving force for the reactions.

Second-order rate constants for the outer-sphere pathway have been determined for $[\mathrm{Co(phen)_3}]^{2+}$ and three derivatives, $[\mathrm{Co(4,7\text{-}Me_2phen)_3}]^{2+}$, $[\mathrm{Co(5,6\text{-}Me_2phen)_3}]^{2+}$, and $[\mathrm{Co(bpy)_3}]^{2+}$ (Table III). The order of the reactivity of the reductants parallels their reduction potentials supporting the assignment of an outer-sphere mechanism. The Marcus theory[55,56] relates the cross-reaction rate constants to the self-exchange rate constants for the reactants and is conveniently expressed in free energy terms as eqs 19 and 20, where ΔG^{**} is the electrostatically corrected free

$$\Delta G_{12}^{**} = \tfrac{1}{2}[\Delta G_{11}^{**} + \Delta G_{22}^{**} + \Delta G^{\circ}(1 + \alpha^{**})] \qquad (19)$$

$$\alpha^{**} = \frac{\Delta G^{\circ}}{4(\Delta G_{11}^{**} + \Delta G_{22}^{**})} \qquad (20)$$

energy of activation[57] and ΔG° is the electrostatically corrected free energy change for the reaction. The self-exchange rates for $[\mathrm{Co(phen)_3}]^{3+/2+}$ and $[\mathrm{Co(bpy)_3}]^{3+/2+}$ under the conditions of the study are known,[15] and values for $[\mathrm{Co(4,7\text{-}Me_2phen)_3}]^{2+}$ and $[\mathrm{Co(5,6\text{-}Me_2phen)_3}]^{2+}$ were obtained by assuming a ionic strength dependence similar to that of the parent $[\mathrm{Co(phen)_3}]^{2+}$. The reagent $[\mathrm{Co(ox)_3}]^{3-/4-}$ has a reduction potential of 0.57 V,[58] but the self-exchange rate is not well-known and is estimated[59,60] variously as 3×10^{-7} $\mathrm{M^{-1}\,s^{-1}}$ or 1.4×10^{-12} $\mathrm{M^{-1}\,s^{-1}}$. In this study a value of 1.2×10^{-8} $\mathrm{M^{-1}\,s^{-1}}$ at 0.017 M ionic strength was calculated from the cross reaction of $[\mathrm{Co(ox)_3}]^{3-}$ with $[\mathrm{Co(phen)_3}]^{2+}$. It compares favorably with a value from the literature[59] of 2.7×10^{-8} $\mathrm{M^{-1}\,s^{-1}}$ when this value is corrected for ionic strength 0.017 M. With use of the self-exchange rate, the rate constants for the reactions of $[\mathrm{Co(ox)_3}]^{3-}$ with $[\mathrm{Co(bpy)_3}]^{2+}$, $[\mathrm{Co(4,7\text{-}Me_2phen)_3}]^{2+}$, and $[\mathrm{Co(5,6\text{-}Me_2phen)_3}]^{2+}$ are calculated to be 57 $\mathrm{M^{-1}\,s^{-1}}$, 850 $\mathrm{M^{-1}\,s^{-1}}$, and 400 $\mathrm{M^{-1}\,s^{-1}}$, in good agreement with the experimentally measured rate constants.

Both inner-sphere and outer-sphere pathways show stereoselectivity. However, the determination of stereoselectivity is complicated by the subsequent racemization of the immediate reaction products in both cases. Analysis of the data by a consecutive reaction scheme is consistent with the assignment of the increase in optical activity to the electron-transfer reactions (eqs 16 and 17), and the subsequent decay to a self-exchange reaction for the outer-sphere pathway, and to the electron-transfer reaction (eq 18) in the case of the inner-sphere pathway. Indeed, there is good agreement between the rates evaluated for these processes from the consecutive reaction treatment of the circular dichroism data and those obtained independently by conventional spectrophotometry. The extent of chiral induction was calculated with use of eq 6.

Inner-sphere stereoselectivity is marked, 63% ΔΔ for $[\mathrm{Co(phen)_2}]^{2+}$ when corrected for the fact that only 91% of the total $[\mathrm{Co(ox)_3}]^{3-}$ is converted to this product under the conditions of the experiment, and 19% ΔΔ for $[\mathrm{Co(bpy)_2}]^{2+}$. These numbers compare with 1.5% ΔΔ for the corresponding reaction of $[\mathrm{Co(en)_2}]^{2+}$.[7] Interpretation of these inner-sphere stereoselectivities is difficult since the mechanism is complex.[61] It is significant that the stereoselectivity increases with the rigidity of the ligand, and this may indicate that formation of the oxalate-bridged intermediate has an important role. In this intermediate, the metals are held ≈5 Å apart so that the chiral ligand chromophores on the two metal ions are not within van der Waals contact distance; however, solvation of the complexes will differ markedly.

Both $[\mathrm{Co(phen)_2(ox)}]^{+}$ and $[\mathrm{Co(bpy)_2(ox)}]^{+}$ racemize rapidly under the conditions of the stereoselectivity experiments, and the mechanisms of this racemization were investigated. In the case of $[\mathrm{Co(phen)_2(ox)}]^{+}$ the reaction with $[\mathrm{Co(phen)_3}]^{2+}$ is sufficient to account almost completely for the racemization reaction. However, in the $[\mathrm{Co(bpy)_2(ox)}]^{+}$ reaction, reduction by $[\mathrm{Co(bpy)_3}]^{2+}$ can account for only 10% of the measured racemization rate. Consequently, a significant contribution from the inner-sphere self-exchange process must be present. It may be that inner-sphere self-exchange occurs also with $[\mathrm{Co(phen)_2(ox)}]^{+}$ but that it has a high stereoselectivity (ΔΔ) resulting in no racemization. Clearly inner-sphere reactions with rigid chiral chromophores may give rise to significant stereoselectivity.

The extent of chiral induction in the outer-sphere reduction of $[\mathrm{Co(ox)_3}]^{3-}$ by $[\mathrm{Co(phen)_3}]^{2+}$ is substantial, 24 ± 1% ΔΔ at 25.0 °C and 0.017 M ionic strength, corresponding to $k_{\Delta\Delta}/k_{\Delta\Lambda} = 1.63$. It is also markedly dependent on the presence of substituents on the reductant ligands. The value for $[\mathrm{Co(bpy)_3}]^{2+}$ is the lowest, reflecting the more flexible nature of this reductant, which renders it less selective than the phenanthroline derivatives. Methyl substituents in the 5,6-positions of the 1,10-phenanthroline ring have little effect on the stereoselectivity compared with the parent complex $[\mathrm{Co(phen)_3}]^{2+}$, while the largest stereoselectivity is observed with $[\mathrm{Co(4,7\text{-}Me_2phen)_3}]^{2+}$.

The outer-sphere pathway follows a complex rate law which suggests the presence of ion-pair formation in solution. In the reaction with $[\mathrm{Co(phen)_3}]^{2+}$, the association constant, $K_0 = 65$ $\mathrm{M^{-1}}$, is of the order of magnitude expected for electrostatic attraction between the −3 and +2 charged ions at 25.0 °C and 0.017 M ionic strength.[62] Thermodynamic parameters are consistent with charge neutralization and substantial release of electrostricted solvent. The subsequent electron-transfer reaction precludes an examination of stereoselectivity in the ion association between $[\mathrm{Co(ox)_3}]^{3-}$ and $[\mathrm{Co(phen)_3}]^{2+}$. A less direct but nevertheless revealing study of ion association by conductivity was carried out on the analogues $[\mathrm{Rh(ox)_3}]^{3-}$ and $[\mathrm{Ru(phen)_3}]^{2+}$. This method allows investigation of chiral recognition in the ion association process by carrying out the measurements with diastereomeric pairs of ions. At 25.0 °C and 0.010 M ionic strength, it is found that $K_0(\Delta\Delta) = 206 \pm 7$ $\mathrm{M^{-1}}$ and $K_0(\Delta\Lambda) = 195 \pm 6$ $\mathrm{M^{-1}}$. There is a small but measurable discrimination favoring the ΔΔ diastereomeric pair. At the higher ionic strength used in the kinetic studies, both the association constants and the chiral discrimination decrease with $K_0 \approx 157$ $\mathrm{M^{-1}}$ and $K_0(\Delta\Delta)/K_0(\Delta\Lambda) = 1.00 \pm 0.03$. The discrimination in favor of the ΔΔ pair decreases with both increasing ionic strength and increasing temperature, suggesting that the ΔΔ pair is more ordered than the ΔΛ pair.[63] Thermodynamic parameters for the chiral recognition, $\Delta\Delta H^{\circ}(\Delta\Delta-\Delta\Lambda) = -1.3 \pm 1.1$ $\mathrm{kJ\,mol^{-1}}$ and $\Delta\Delta S^{\circ}(\Delta\Delta-\Delta\Lambda) = -4.3 \pm 3.5$ $\mathrm{J\,K^{-1}\,mol^{-1}}$, are not particularly well defined but are consistent with

---

(55) Marcus, R. A. *Annu. Rev. Phys. Chem.* **1964**, *15*, 155–196.

(56) Newton, M. D.; Sutin, N. *Annu. Rev. Phys. Chem.* **1984**, *35*, 437–480.

(57) Brown, G. M.; Sutin, N. *J. Am. Chem. Soc.* **1979**, *101*, 883–892.

(58) Hin-Fat, L.; Higginson, W. C. E. *J. Chem. Soc. A* **1967**, 298–301.

(59) Holwerda, R. A.; Knaff, D. B.; Gray, H. B.; Clemmer, J. D.; Crowley, R.; Smith, J. M.; Mauk, A. G. *J. Am. Chem. Soc.* **1980**, *102*, 1142–1146.

(60) Ehighaokhuo, J. O.; Ojo, J. F.; Olubuyide, O. *J. Chem. Soc., Dalton Trans.* **1985**, 1665–1667.

(61) Bernauer, K.; Pousaz, P.; Porret, J.; Jeanguenat, A. *Helv. Chim. Acta* **1988**, *71*, 1339–1348.

(62) Fuoss, R. M. *J. Am. Chem. Soc.* **1958**, *80*, 5059–5061.

(63) Although the value for the ion association constant obtained by this method is a factor of 2 higher than the value obtained from the kinetic study, the system provides a reasonable model for the interaction of $[\mathrm{Co(ox)_3}]^{3-}$ and $[\mathrm{Co(phen)_3}]^{2+}$. The discrepancy reflects a compromise between the choice of value for the equivalent conductance of the ion pair and ambiguities inherent in the kinetic rate law.

Table VII. Selected Activation Parameters for Intramolecular Electron Transfer

reductant	oxidant	*I*, M	ΔH_{et}^{*}, kJ mol^{-1}	ΔS_{et}^{*}, J K^{-1} mol^{-1}	ref
$[Co(phen)_3]^{2+}$	$[Co(ox)_3]^{3-}$	0.017	32	−148	this work
$[Fe(CN)_6]^{4-}$	$[Co(NH_3)_5N_3]^{2+}$	1.0	104	+44	64
$[Fe(CN)_6]^{4-}$	$[Co(NH_3)_5(Me_2SO)]^{3+}$	1.0	84	+25	64
$[Fe(CN)_6]^{4-}$	$[Co(NH_3)_5(py)]^{3+}$	1.0	118	+113	64
PCu(I)	$[Co(phen)_3]^{3+}$	0.1	18	−163	65
$(NH_3)_5Ru(II)$–cyt *c*(III)		0.28	15	−163	66
$[(NH_3)_5Os–(iso(Pro)_3)–Ru(NH_3)_5]^{5+}$		0.2	31	−96	67
$[(SO_4)(NH_3)_4Ru–(iso(Pro)_3)–Co(NH_3)_5]^{3+}$		0.95	61	−121	68
$[(SO_4)(NH_3)_4Ru–(iso(Gly)_2)–Co(NH_3)_5]^{3+}$		1	56	−155	69

this suggestion. It can be concluded that the chiral recognition in ion pairing in this model system is insufficient to explain the induction observed in the overall electron-transfer reaction. Clearly, the bulk of the selectivity must arise from some other source.

The ion-pair assembly is envisaged as a dynamic, equilibrium distribution of the ions in many different configurations. This distribution was investigated by ^{1}H NMR relaxation experiments on the model system involving the diamagnetic analogue $[Co(phen)_3]^{3+}$ in the presence of the paramagnetic probe $[Cr(ox)_3]^{3-}$. Although the charge product for the model ion pair is increased by three over that in the electron-transfer reaction, similar studies with $[Ru(phen)_3]^{2+}$ as the diamagnetic complex proved impossible due to precipitation in the presence of $[Cr(ox)_3]^{3-}$. The relaxation experiments reflect the fact that the ion pairs formed between these two complexes are labile and have a large component of indeterminate or random structure. However, there is a predominance of configurations with approach along the C_3 axis of $[Co(phen)_3]^{3+}$. It must be emphasized that the structure which is evaluated is not static but a dynamic average of many different configurations. On average for the structured configurations, the paramagnetic center is to be found close to the C_3 axis of $[Co(phen)_3]^{3+}$ with a Cr–Co distance around 5.9 Å (Figure 8). Comparisons with the X-ray structure of $K(\Delta\text{-}[Ni(phen)_3])(\Delta\text{-}[Co(ox)_3])\cdot 2H_2O$, which shows the ions with a mutual C_3–C_3 interaction and a Co–Ni distance of 6.1 Å, are striking and give credence to the NMR model. This structure can be rationalized as the approach along mutual C_3 axes represents the smallest metal–metal distance and, hence, the largest electrostatic attraction. From the NMR results, it is estimated that the structured component of the ion pair contributes around 30% to the total population.[54] Despite this evidence for a structured interaction, the conductivity studies reveal that ion pairing involves little chiral recognition.

In the reaction between $[Co(ox)_3]^{3-}$ and $[Co(phen)_3]^{2+}$, the limiting electron-transfer rate constant, $k_{et} = 0.24 \pm 0.07$ s^{-1}, is slow and consequently represents reaction within an equilibrium distribution of configurations, each of which has its individual rate constant for electron transfer.[56] Some configurations will be favorable for electron transfer, and some will not. A comparison of the activation parameters with values for other well-defined intramolecular electron-transfer processes is presented in Table VII. In the reaction between $[Co(ox)_3]^{3-}$ and $[Co(phen)_3]^{2+}$, ΔH_{et}^{*} is modest and ΔS_{et}^{*} is strongly unfavorable, contrasting with reductions of complexes such as $[Co(NH_3)_5(OSMe_2)]^{3+}$ by $[Fe(CN)_6]^{4-}$, where the activation enthalpies are larger and the activation entropies are favorable. Large unfavorable activation entropies are noted for intramolecular electron transfer involving inorganic complexes and the redox centers of metalloproteins and are thought to be a characteristic of a nonadiabatic process. However, the activation parameters are also consistent with a high degree of discrimination for electron transfer within the assembly of ion-pair configurations, and this interpretation is preferred in the present case.

Although chiral recognition in the ion pair is relatively unimportant, chiral induction in the overall electron-transfer reaction is significant. Specifically, there is a preference for electron transfer within ΔΔ ion pairs. The NMR studies in conjunction with crystallographic data suggest that the dominant interaction involves a mutual C_3–C_3 orientation of the reactants. It can be argued that the dominant ion-pair structure may bear no relation to the structure required for the electron-transfer precursor. However, it is more difficult to argue that substantial stereoselectivity can arise from a random or spherically symmetric interaction, and hence, the structured component of the ion pair is likely to contribute to the chiral induction. Partial support for this lies with the limited data on electron-transfer stereoselectivity for structural variants of $[Co(phen)_3]^{2+}$. The stereoselectivity is small, 5% ΔΔ, for $[Co(bpy)_3]^{2+}$, which is more flexible than $[Co(phen)_3]^{2+}$. For $[Co(5,6\text{-}Me_2phen)_3]^{2+}$, the additional methyl groups do not interfere with the C_3 axis and have little effect on the stereoselectivity, but with $[Co(4,7\text{-}Me_2phen)_3]^{2+}$, where the stereoselectivity is largest, the methyl groups surround the C_3 axis and enhance the discrimination along this axis. One explanation for the chiral induction is provided by the moderating influence that ligand orbitals may have on the electron transfer. In the C_3–C_3 structured ΔΔ-ion pair, the π-orbitals of the 1,10-phenanthroline ligands of $[Co(phen)_3]^{2+}$ and the oxalate ligands of $[Co(ox)_3]^{3-}$ lie parallel and may have better overlap than in the ΔΛ-ion pair where they are almost orthogonal. It seems likely that greater reorganization in the ΔΛ-ion pair will be required as a result of this poorer orbital overlap. Activation parameters for the chiral induction, $\Delta\Delta H_{et}^{*}(\Delta\Delta - \Delta\Lambda) = -1.8 \pm 1.2$ kJ mol^{-1} and $\Delta\Delta S_{et}^{*}(\Delta\Delta - \Delta\Lambda) = -2.1 \pm 3.8$ J K^{-1} mol^{-1}, show that electron transfer in the more ordered ΔΔ-ion pair is favored enthalpically, most likely the result of outer-sphere reorganization.

In conclusion, the stereoselectivity results strongly suggest that the electron-transfer process discriminates between different configurations of the reactants. In light of this observation it is initially surprising that the reactions show a large degree of self-consistency with the Marcus approach. However, the interactions between $[Co(ox)_3]^{3-}$ and the four reductants are expected to be similar, resulting in considerable internal consistency.

Acknowledgment. The support of the National Science Foundation (Grant No. CHE 90-16682) is gratefully acknowledged.

Supplementary Material Available: Lists of pseudo-first-order rate constants (Tables SI and SII) (5 pages). Ordering information is given on any current masthead page.

---

(64) Krack, I.; van Eldik, R. *Inorg. Chem.* **1990**, *29*, 1700–1704.

(65) Segal, M. G.; Sykes, A. G. *J. Am. Chem. Soc.* **1978**, *100*, 4585–4592.

(66) Isied, S. S.; Kuehn, C.; Worosila, G. *J. Am. Chem. Soc.* **1984**, *106*, 1722–1726.

(67) Vassilian, A.; Wishart, J. F.; van Hemelryck, B.; Schwarz, H.; Isied, S. S. *J. Am. Chem. Soc.* **1990**, *112*, 7278–7286.

(68) Vassilian, A.; Isied, S. S. *J. Am. Chem. Soc.* **1984**, *106*, 1732–1736.

(69) Vassilian, A.; Isied, S. S. *J. Am. Chem. Soc.* **1984**, *106*, 1726–1732.